Materials Science Forum Vols. 389-393 (2002) pp. 613-616

Photoconductivity of Lightly-Doped and Semi-Insulating 4H-SiC and the Free Exciton Binding Energy

I.G. Ivanov, J. Zhang, L. Storasta and E. Janzén

Department of Physics and Measurement Technology, Linköping University, SE-581 83 Linköping, Sweden

Keywords: Electronic Band-Gap, Exciton Binding Energy, Excitonic Band-Gap, Extrinsic Photocurrent, Intrinsic Photocurrent

Abstract. The paper presents a study of the structure of the photoconductivity spectra of various 4H-SiC samples near the absorption edge. By means of comparison of the spectra of low doped (mid 10^{14} cm^{-3}), very low doped (in 10^{13} cm^{-3} range), and semi-insulating moderately doped samples, features in the photocurrent due to contribution from creation of free carriers (i.e., excitons in the continuum) can be recognised. This is used for determination of the free exciton binding energy, 20.5 ± 1 meV, in agreement with a previous study. The second lowest conduction band and the spin-orbit split off valence band are also detected.

Introduction

The free-exciton (FE) binding energy, E_{bx}, is a fundamental parameter, however, its exact value is far from being well established in any of the SiC polytypes. Values obtained in previous studies often do not agree (see Ref. [1] for a review), which determines the need for further experimental work employing techniques different from those used before. In a recent paper (Ref. [2]) we demonstrated the use of photoconductivity (PC) for studying the structure of the exciton absorption edge, and reported on the determination of E_{bx} in 6H-SiC. The purpose of the present work is to use a similar approach for studying the structure of the excitonic bands in 4H-SiC. This will include the determination of the FE binding energy, as well as the further development of the interpretation of the PC spectrum near the fundamental absorption edge.

The basic idea behind the application of PC for finding the position of the conduction band edge (which coincides with the edge of the exciton continuum) is discussed in Ref.[2]. In brief, since excitons are electrically neutral, no contribution to the photocurrent from free excitons is expected, if the excitons are created by the exciting light in bound states (below the exciton continuum). However some current is anticipated if they are created in the continuum of non-bound states. In the latter case, the electron and hole can be separated in the applied electric field before they form an exciton in a bound state, and thus contribute to the photocurrent. The threshold of this intrinsic photocurrent is at the conduction band edge E_g plus the lowest energy ($\hbar\Omega_0$) of a phonon insuring the momentum conservation in the light absorption process.

However, in real samples the threshold of the photocurrent occurs at the fundamental absorption edge (i.e., the excitonic bandedge plus $\hbar\Omega_0$). Thus even excitons created in bound states contribute to the photocurrent via capturing and Auger recombination at impurities (extrinsic photocurrent). This process usually dominates, so the intrinsic photocurrent is obscured. However, in samples of exceptionally low residual doping, the extrinsic photocurrent is seen to saturate closely above the absorption edge, which enables the observation of the intrinsic counterpart in the current. The thresholds in the intrinsic photocurrent are identified as due to the involvment of different momentum-conserving phonons in the absorption process, which enables the determination of the free-exciton binding energy.

Samples and Experimental Details

Three kinds of 4H-SiC samples were investigated, referred to as sample A [low-doped epitaxial layer (n ≈ 3 to 4 10^{14} cm^{-3}), grown by conventional hot-wall CVD technique]; sample B [very low-doped (n in 10^{13} cm^{-3} region), grown in a vertical hot-wall (chimney) reactor], and sample C [semi-insulating (SI) bulk 4H-SiC with moderate residual doping grown in high-growth rate HTCVD reactor]. The substrate was polished away from the epitaxial layers. The photocurrent was excited by either a Xe-lamp passed through a high-resolution monochromator with excitation spectral linewidth between 2.5 and 5 Å, or a dye-laser with linewidth below 0.1 Å. In the latter case the highest excitation energy was limited to about 3360 - 3370 meV, still covering a significant part of the spectrum near the absorption edge.

Results and Discussion

The PC spectrum for sample A is shown in Fig.1. This spectrum is also representative for highly doped samples (e.g., n-type substrates, not shown here). Its main features are similar to those of the absorption spectrum [3], and comprise thresholds corresponding to phonon assisted absorption of a photon to create an exciton at the bottom of the lowest energy excitonic band. Each threshold consists of two steps (therefore double arrows in Fig.1). The low energy step (weaker) corresponds to creation of excitons with holes from the top of the valence band, and the stronger step involves holes from the next valence band split-off by spin-orbit interaction. From our measurements, the value of the splitting can be estimated to 7 - 8 meV. It has been estimated theoretically to 10 meV (Ref. [4]), and measured as 6.8 ± 0.6 meV by wavelength modulation spectroscopy [5], with which our value is obviously in agreement.

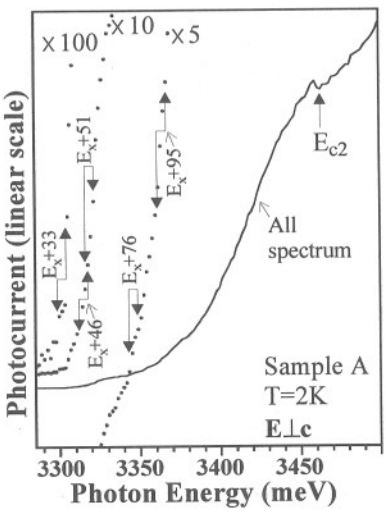

Fig.1. PC spectrum of higher-doped sample A (solid line). In order to reveal the thresholds discussed in the text, the experimental points are shown for some parts of the spectrum, scaled as denoted and shifted to fit the frame. E_{c2} denotes the second lowest conduction band (see text).

The excitons created within the exciton band contribute to the photocurrent via capturing to and Auger recombination at impurities, as discussed in Ref.[2]. The same phonons as those responsible for the appearance of phonon replicas (of either bound or free exciton related emission) in the usual photoluminescence (PL) spectrum are involved. Similar to the absorption spectrum, the phonons that couple strongly to photons and produce intense phonon replicas in the PL spectrum produce also higher steps (thresholds) in the PC spectrum (some of the phonons are denoted by their energies in meV in Fig.1, e.g. the 33 meV phonon gives rise to the threshold starting at energy E_x+33 meV = 3298 meV, etc.). To conclude, the spectrum in Fig.1 is completely dominated by extrinsic (i.e., due to Auger recombination at impurities) photocurrent.

Fig.2a shows the corresponding spectrum for the very low-doped sample B. The initial part of the spectrum near the absorption edge exhibits the same features at 33 and 46 meV phonon-assisted thresholds, however, at higher energies, the extrinsic photocurrent saturates, and even decreases in the interval approximately 3340 - 3360 meV. This enables the observation of the intrinsic photocurrent. Its threshold is anticipated at energy $E_g + \hbar\Omega_0$, where E_g is the electronic bandgap (coinciding with the exciton continuum). Since the lowest energy 33 meV phonon in 4H-SiC couples only very weakly to the light, one should try to identify first the strongly coupling

phonons with energies 46 and 76 meV. We assign the thresholds visible in the spectrum (Fig.2a) at about 3332 meV and 3362 meV to transitions to the conduction band assisted by the 46 and 76 meV phonons, respectively. Furthermore, the threshould around 3350 - 3355 meV, seen in the derivative, matches rather well (in position and oscillator strength) to transition assisted by the 68 meV phonon. This data suggests a free exciton binding energy $E_{bx} = E_g - E_x \approx 20$ meV. The attribution of the features at 3332 and 3362 meV to intrinsic photocurrent is supported by the spectrum of a semi-insulating sample, shown in Fig.2b. Similar to the spectrum in Fig.2a, the photocurrent saturates and starts decreasing around 3330 - 3340 meV. (The mechanism responsible for the saturation is not currently understood, but most probably it is related to the compensation present in both samples, and *not* to the low doping level, as previously suggested in Ref.[2].) However, unlike sample B, the spectrum of sample C completely lacks the structures attributed to intrinsic photocurrent (confer also the derivatives), which is to be expected in view of the significantly higher doping level of the semi-insulating bulk substrate (sample C), as well as the complete absence of free-exciton related emission in the usual low-temperature PL from that sample. It is worth noting also the threshold at 3460 meV (well visible in Fig.1 and Fig.2a), coinciding with a feature in the absorption spectrum measured in Ref. [6] and attributed to transition into a higher lying conduction band E_{c2}. If one assumes that the "strongest" 76 meV phonon assists the transition into E_{c2}, one obtains that this band is positioned about 105 meV above the conduction band E_g (E_g = 3285 meV = $E_x + E_{bx}$). This value is in fairly good agreement with the value of 120 meV calculated in [4].

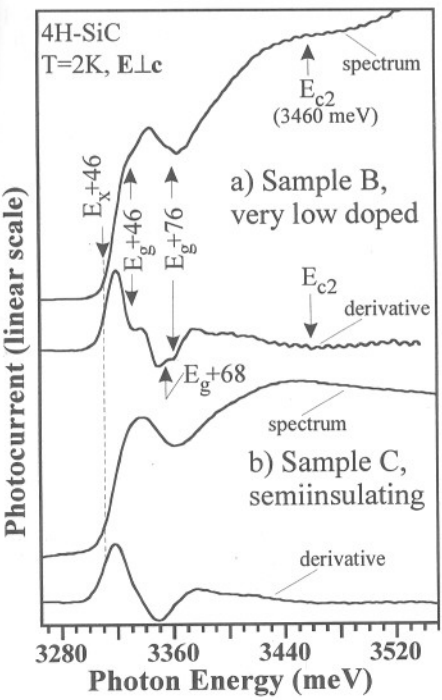

Fig.2. Comparison of the PC spectra of sample B and C. The derivatives of each spectrum ar displayed below it. The notations of the thresholds are similar to those in Fig.1, E_g denote the electronic bandgap (the exciton continuum).

The use of Xe-lamp + monochromator excitation limits the resolution (5Å in Fig.1 and 2.5 Å in Fig.2). The spectra in Fig.3 (sample B) were recorded using tuneable dye-laser excitation for both polarizations of the laser with respect to the crystal axis **c**. The interference pattern visible in the spectrum in Fig.3a (**E** ⊥ **c**) is from the sample (the period corresponds to normal incidence on of the 70 μm thick sample). Still, after smoothing the derivative can be calculated. It exhibits the same structure as the derivative in Fig. 2a, thus confirming the previous assignment. Note that the increase in the intrinsic photocurrent around 3662 meV corresponding to E_g + 76 meV is only observed in the derivative, not directly in the original spectrum (cf. Fig.2), probably due to the rapidly decreasing power of the dye laser in this region.

The spectrum measured with **E** || **c** polarization (Fig.3b) shows the following features. Firstly, the peak in the photocurrent occurs at slightly lower energy, and the decrease is stronger. The most probable reason for the faster decrease is the decrease of the penetration depth of the laser with the increase of the absorption. [Note the sharp decrease of the photocurrent above 3342 meV (= E_x + 76 meV), where sharp increase of the absorption is expected.] Secondly, owing to the lack of interference in this configuration, new thresholds of the intrinsic photocurrent can be resolved, marked E_g+41 and E_g+68 in Fig.3b (similar to E_x+41 originating from the *extrinsic* counterpart in Fig.3b). These new features correspond very well to the phonons with energies 40.6 - 41.9 meV and

68.8 meV coupling to light **E** || **c** (see Ref.[7]). There is some contribution in the spectrum from **E**⊥**c** polarization (not marked in Fig.3b). The thresholds in the intrinsic photocurrent in the **E**|| **c** configuration are consistent with $E_{bx} \approx 20$ meV.

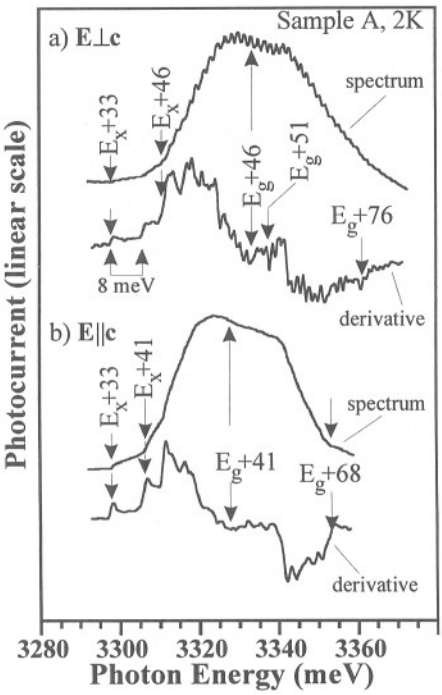

Fig.3. Laser excited spectra of sample B, obtained with **E** ⊥ **c** (a) and **E**|| **c** (b) polarizations of the laser. Same notations as in Fig.1 and 2 are used, the derivatives are shown below each spectrum.

Conclusion

The experimental data considered in this paper allows us to conclude, that the free exciton binding energy in 4H-SiC can be estimated to E_{bx} = 20.5 ± 1 meV. The value is in agreement with the previously reported value in Ref.[8]. A theoretical estimate based on the isotropic hydrogenic model for 4H-SiC yields the value 34 meV, however, such calculation has very limited accuracy due to the high anisotropy of the electron and hole effective masses in 4H-SiC. Precise calculations accounting for this anisotropy are not currently available.

Certain structures in the spectra yield the value of the valence band spin-orbit splitting (7.5 ± 0.5 meV), and the position of the second conduction band, lying about 105 meV above E_g, where the electronic bandgap at T = 2K is $E_g \approx$ 3285 meV, according to this paper.

Acknowledgements.
Support from the Swedish Research Council, the SSF Program SiCEP, Okmetic, ABB and ABB Corporate Research is gratefully acknowledged.

References

[1] R.P. Devaty and W.J. Choyke, phys. stat. sol. (a) **162**, 5 (1997).

[2] I.G. Ivanov, T. Egilsson, J. Zhang, A. Ellison and E. Janzén, Proc. of the 3rd European Conference on Silicon Carbide and Related Materials (Kloster Banz, Germany, September 2000), Trans Tech Publications, Switzerland, 2001, p.405.

[3] W.J. Choyke, Mat. Res. Bull. **4**, 141 (1969).

[4] C. Persson, U. Lindefelt, J. Appl. Phys. **82**, 5496 (1997).

[5] S.G. Sridhara, S. Bai, O. Shigiltchoff, R.P. Devaty, W.J. Choyke, Proc. of the ICSCRM '99; Research Triangle Park, NC, USA; 10-15 Oct., 1999; Mater. Sci. Forum **338-342**, 567 (2000).

[6] S.G. Sridhara, T.J. Eperjesi, R.P. Devaty, W.J. Choyke, Proc. of the 2nd ECSCRM; Montpellier, France; Sept. 2-4, 1998; Mater. Sci. Eng. **B61-62**, 229 (1999).

[7] I. G. Ivanov, U. Lindefelt, A. Henry, O. Kordina, C. Hallin, M. Aroyo, T. Egilsson, E. Janzén, Phys. Rev. B **58**, 13634 (1998).

[8] G.B. Dubrovskii and V.I. Sankin, Soviet Phys. - Solid State **17**, 1847 (1975).